

## Driven Diffusion of Confined Polymers

Jae Youn Lee and Roger F. Loring\*

Department of Chemistry and Chemical Biology,  
Baker Laboratory, Cornell University,  
Ithaca, New York 14853

Received March 5, 2001

Revised Manuscript Received May 15, 2001

### Introduction

Fluids confined on molecular length scales display differing structure and dynamics from bulk systems. Depending upon the nature of the liquid and of the confining surfaces, confinement may either enhance or reduce molecular mobility and relaxation.<sup>1–5</sup> Manias et al.<sup>6</sup> have recently reported X-ray diffraction and small-angle neutron scattering measurements of the intercalation dynamics of polystyrene from the melt into the 2 nm galleries of alkylammonium ion exchanged fluorohectorite, a mica-type layered silicate.<sup>7</sup> These studies permit the determination of a nonequilibrium diffusion coefficient, denoted here  $D_{\text{neq}}$ , that characterizes the transport of polymer from the bulk into a confining structure. The data support three primary conclusions.<sup>6</sup> First,  $D_{\text{neq}}$  is found to be substantially larger than the polymer self-diffusion coefficient in an equilibrium bulk melt. Second, increasing the polymer's affinity for the silicate surface slows the intercalation process. Third,  $D_{\text{neq}}$  is found to scale with chain length,  $N$ , as  $D_{\text{neq}} \propto N^{-1}$ , for polystyrene of molecular weight 2–52  $M_e$  (the entanglement molecular weight), over which range the equilibrium, bulk self-diffusion coefficient scales<sup>8</sup> as  $N^{-2}$ , as in the reptation picture.

To model the formation kinetics of polymer-layered silicate nanocomposites, we have performed<sup>9–12</sup> molecular dynamics simulations of the flow of polymer from a bulk melt into a slit. These calculations are consistent with the first two experimental observations above: that  $D_{\text{neq}}$  is significantly larger than the equilibrium, bulk self-diffusion coefficient and that increasing polymer–surface attractive interactions decreases  $D_{\text{neq}}$ .<sup>9–11</sup> Here we address the third experimental finding of the  $N$  dependence of  $D_{\text{neq}}$ .

Manias et al.<sup>6</sup> interpret the  $N$  dependence of  $D_{\text{neq}}$  with an argument developed by Valignat et al.<sup>13</sup> for the spreading of the precursor film of a polymer droplet on a solid surface.<sup>14</sup>  $D_{\text{neq}}$  is represented as

$$D_{\text{neq}} \approx \frac{\Delta G}{\zeta} \quad (1)$$

with  $\Delta G$  the free energy difference per molecule in the intercalated and bulk phases and  $\zeta$  a friction coefficient characterizing the polymer dynamics in the slit.  $\Delta G$  is conjectured to scale linearly<sup>6,13</sup> with  $N$ , leading to the conclusion that the friction coefficient characterizing the intercalated phase scales as  $N^2$ . To separate the  $N$  dependences of  $\Delta G$  and  $\zeta$  in eq 1, we consider the self-diffusion of confined polymers at equilibrium in the slit with diffusion coefficient  $D_{\text{eq}} \propto k_B T / \zeta$ . If the  $N$  dependence of  $\zeta$  is identical for equilibrium and nonequilibrium dynamics, then

$$D_{\text{neq}}/D_{\text{eq}} \propto \Delta G/k_B T \quad (2)$$

and the  $N$  dependences of  $\Delta G$  and  $\zeta$  may be determined separately by computing  $D_{\text{eq}}$  and  $D_{\text{neq}}$ .

### Results and Conclusions

We first establish that the simulation model of refs 11 and 12 is consistent with the laboratory observation<sup>6</sup> that  $D_{\text{neq}} \propto N^{-1}$ . The model is described fully in ref 11 and summarized briefly here. The simulation cell is divided into three compartments, as shown in Figure 1 of ref 11, with two outer compartments providing reservoirs of bulk polymer melt and an inner compartment containing a slit with walls subject to fixed external pressure. Attached to the slit walls are grafted chains, representing the alkylammonium surfactants in the organically modified fluorohectorite. Both polymer and surfactant molecules are represented by the Kremer–Grest model of bead–spring chains,<sup>15</sup> with grafted chains having 12 beads and polymers having a variable number  $N$  beads. The diameter and mass of polymer (p) and surfactant (s) beads are related through  $\sigma_s = 0.6\sigma_p$  and  $m_s = 0.216m_p$ . A constant pressure of  $p = 5.2 \epsilon\sigma_p^{-3}$  is applied to both the slit walls and the polymer reservoirs, the system is coupled to a Brownian heat bath<sup>9,15</sup> to maintain the temperature at  $k_B T/\epsilon = 1.0$ , and the initial monomer density in the reservoirs is  $\rho = 0.85\sigma_p^{-3}$ . Nonbonded interactions between polymer beads are purely repulsive, truncated<sup>11</sup> Lennard-Jones interactions with energy parameter,  $\epsilon$ . Nonbonded interactions between surfactant beads have the same form, as do interactions between surfactant and polymer beads and surfactant beads and the immobile particles composing the slit walls. Slit walls are composed of a rigid fcc lattice of particles whose interaction with polymer beads is of the Lennard-Jones form with an attractive tail<sup>11</sup> and energy parameter,  $3\epsilon$ . We simulate the intercalation process by equilibrating polymer and organically modified silicate separately and then allowing the polymer access to the slit, with intercalation, if spontaneous, proceeding at constant pressure.<sup>11,12</sup>

We examine the squared displacements along the slit axis of individual polymer beads as they enter the slit. We follow the convention of Figure 1 of ref 11 and denote the flow direction along the slit axis  $x$  and the direction along which the slit opens  $z$ . The monomer mean-squared displacement along  $x$ , averaged over all beads in the slit on time scales before the two propagating polymer fronts have met, is found to grow linearly with time, permitting the definition of  $D_{\text{neq}}$  by  $\langle x^2(t) \rangle = 2D_{\text{neq}}t$ . Our definition of a nonequilibrium diffusion coefficient in terms of molecular mean-squared displacements is based on the empirical observation, shown in Figure 4 of ref 9, that for polymer flow into a slit a diffusion coefficient defined by mean-squared displacements of individual molecules has a very similar magnitude to a nonequilibrium diffusion coefficient defined in terms of the time dependence of the total amount of intercalated material. The latter definition is employed to analyze laboratory data in ref 6. Diffusion coefficients based on both of these definitions are compared with nonequilibrium diffusion coefficients based on determination of fluxes of polymer beads in ref 9.

$D_{\text{neq}}$  is plotted in Figure 1 for polymer chains of length  $N = 12, 24, 36$ , and 72 and is fit to  $D_{\text{neq}} \propto N^{-0.95}$ . The initial slit width<sup>11</sup> is  $3.2\sigma_p$ , and the slit width at the end

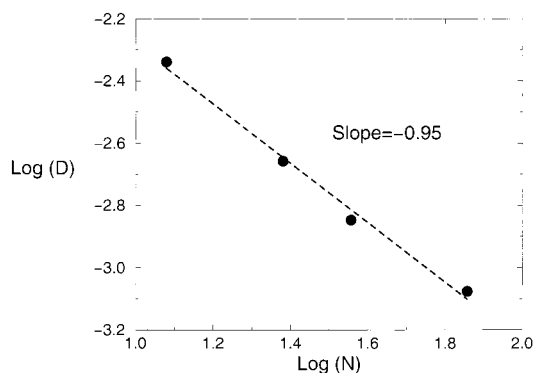


**Figure 1.** Dependence of the nonequilibrium diffusion coefficient  $D_{\text{neq}}$  on chain length  $N$  is shown for flow of polymer from the bulk into a confining slit with grafted surfactants maintained at constant pressure.  $D_{\text{neq}} \propto N^{-1}$ , even for  $N > N_e \approx 35$ .

of the simulations is  $4.2\sigma_p - 4.4\sigma_p$  for  $N = 12, 24$ , and  $36$  and is  $3.6\sigma_p$  for  $N = 72$ . For the Kremer–Grest model of an equilibrium bulk melt, the entanglement length is  $N_e \approx 35$ , with  $N = 72$  in the regime of entangled dynamics. Figure 1 suggests that the scaling  $D_{\text{neq}} \propto N^{-1}$  persists for  $N > N_e$ , as observed in the laboratory.<sup>6</sup> For equilibrium diffusion in the bulk melt, Kremer and Grest<sup>15</sup> showed that significant deviations from  $N^{-1}$  scaling occurred for  $N > 50$ . Simulations for a range of  $N$  with  $N > 72$  would be required to obtain a definitive conclusion. Together with eq 1 and the conjecture that  $\Delta G \propto N$ , this result implies  $D_{\text{eq}} \propto N^{-2}$ . This prediction is qualitatively consistent with our previous finding<sup>11</sup> that during intercalation most of the polymer beads are adsorbed to the slit walls, suggesting that chains may reptate among surfactant grafting sites. Confirming this prediction by direct computation of  $D_{\text{eq}}$  for the filled slit is made difficult by the slow dynamics of the confined polymer at equilibrium, especially for  $N > N_e$ .

Instead, we test eq 2 for two simplified versions of the present model that are more amenable to simulation under equilibrium conditions. In these models, polymer from a single bulk reservoir maintained at constant pressure  $p = 5.2\epsilon\sigma_p^{-3}$  with density  $\rho = 0.85\sigma_p^{-3}$  enters a slit of fixed volume and length greater than  $90\sigma_p$  without grafted surfactants.<sup>9,10</sup> As in the model described above, the silicate is represented by a rigid fcc lattice of immobile particles. Polymer–polymer interactions remain as described above (purely repulsive truncated Lennard-Jones potential<sup>11</sup>), but the polymer–silicate interactions have energy parameter  $\epsilon$ , rather than  $3\epsilon$ , as above. The model including grafted chains and a slit under constant pressure requires a greater polymer–silicate attraction for spontaneous intercalation than do the present models with fixed slit volume. The effect of increasing the polymer–silicate attraction is discussed in ref 10. In the first model, polymer flows into an initially evacuated slit, formed by removing two central layers of the fcc lattice, producing a channel of width<sup>9,10</sup>  $2.9\sigma_p$ , measured between the centers of the lattice particles forming the walls. In the second model, the slit contains obstacles, resulting from the partial removal of the two central layers of the fcc lattice, leaving behind two lattice planes containing rectangular lattices of immobile particles, with in-plane lattice constants of  $2.4\sigma_p$  along  $x$  and  $2.1\sigma_p$  along  $y$ . The surface density of obstacles in each plane is  $0.17\sigma_p^{-2}$ , corresponding to a bulk obstacle density in the slit of  $\rho = 0.18\sigma_p^{-3}$ .

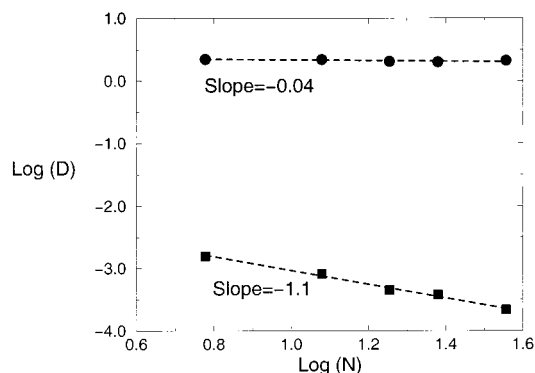


**Figure 2.** Chain length dependence of the nonequilibrium diffusion coefficient  $D_{\text{neq}}$  (filled circles) and of the equilibrium self-diffusion coefficient  $D_{\text{eq}}$  (filled squares) is shown for an initially evacuated slit.

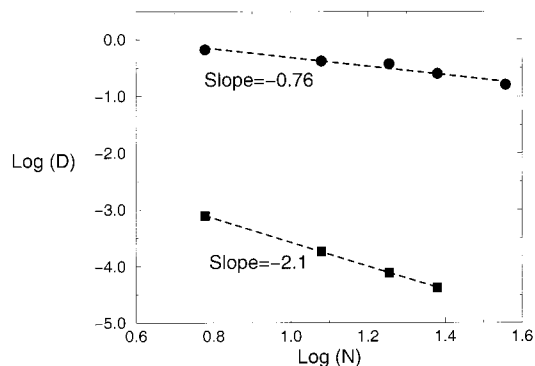


**Figure 3.** Chain length dependence of the nonequilibrium diffusion coefficient  $D_{\text{neq}}$  (filled circles) and of the equilibrium self-diffusion coefficient  $D_{\text{eq}}$  (filled squares) is shown for a slit containing immobile obstacles.

Figure 2 shows the  $N$  dependence of  $D_{\text{neq}}$  and  $D_{\text{eq}}$  for the initially evacuated slit of fixed volume, with  $N = 6, 12, 18, 24$ , and  $36$ .  $D_{\text{neq}}$  is determined as in Figure 1 by computing  $\langle x^2(t) \rangle$  of polymer beads flowing into the slit, and  $D_{\text{eq}}$  is determined by the same procedure for equilibrated polymer inside the slit.  $D_{\text{neq}}$  is nearly independent of  $N$ , with  $D_{\text{neq}} \propto N^{-0.04}$ , while  $D_{\text{eq}} \propto N^{-1.1}$ . Equations 1 and 2 imply that for this model  $\Delta G \propto N^{1.1}$  and  $\zeta \propto N^{1.1}$ . Figure 3 shows the corresponding analysis for the model of a slit containing immobile obstacles for  $N = 6, 12, 18, 24$ , and  $36$  in the nonequilibrium case and for  $N = 6, 12, 18$ , and  $24$  in the equilibrium case. Here  $D_{\text{neq}} \propto N^{-0.76}$  and  $D_{\text{eq}} \propto N^{-2.1}$ , implying that  $\Delta G \propto N^{1.3}$  and  $\zeta \propto N^{2.1}$ . We expect these scalings to vary with the strength of polymer–silicate attractive interactions, as observed in the laboratory for the spreading of a polymer liquid on a solid surface by Valignat.<sup>13</sup> For example, redoing the calculation in Figure 3 with the polymer–silicate interaction energy increased from  $\epsilon$  to  $3\epsilon$  results in  $D_{\text{neq}}$  more closely approximating  $N^{-1}$  scaling.

The calculations in Figures 2 and 3 are approximately consistent with the conjecture  $\Delta G \propto N$ . They support the notion that  $\zeta \propto N$  for confined polymers in the absence of obstacles, as in the Rouse model,<sup>16</sup> while  $\zeta \propto N^2$  for confined polymers in the presence of obstacles as in a reptation model for bulk polymers.<sup>17</sup> These results provide empirical support for the application of eq 1 to intercalation kinetics and for the general relationship between equilibrium and driven diffusion of confined polymers in eq 2. The conjecture<sup>6</sup>  $\zeta \propto N^2$  for polymer motion in layered silicates is consistent with

the equilibrium dynamics of confined polymers among obstacles, which may represent the effects of grafted surfactants and adsorbed polymers.

**Acknowledgment.** This work was supported by the Cornell Center for Materials Research (CCMR), a Materials Research Science and Engineering Center of the National Science Foundation (DMR-0079992).

## References and Notes

- (1) Bhushan, B.; Israelachvili, J.; Landman, U. *Nature (London)* **1995**, *374*, 607.
- (2) Demirel, A.; Granick, S. *Phys. Rev. Lett.* **1996**, *77*, 2261.
- (3) Jerome, B.; Commandeur, J. *Nature (London)* **1997**, *386*, 589.
- (4) Anastasiadis, S. H.; Karatasos, K.; Vlachos, G.; Manias, E.; Giannelis, E. P. *Phys. Rev. Lett.* **2000**, *84*, 915.
- (5) Zax, D. B.; Yang, D. K.; Santos, R. A.; Hegemann, H.; Giannelis, E. P.; Manias, E. *J. Chem. Phys.* **2000**, *112*, 2945.
- (6) Manias, E.; Chen, H.; Krishnamoorti, R.; Genzer, J.; Kramer, E. J.; Giannelis, E. P. *Macromolecules* **2000**, *33*, 7955.
- (7) Giannelis, E. P. *Adv. Mater.* **1996**, *8*, 29.
- (8) Green, P. F.; Palmstrom, C. J.; Mayer, J. W.; Kramer, E. J. *Macromolecules* **1985**, *18*, 501.
- (9) Lee, J. Y.; Baljon, A. R. C.; Loring, R. F.; Panagiotopoulos, A. Z. *J. Chem. Phys.* **1998**, *109*, 10321.
- (10) Baljon, A. R. C.; Lee, J. Y.; Loring, R. F. *J. Chem. Phys.* **1999**, *111*, 9068.
- (11) Lee, J. Y.; Baljon, A. R. C.; Loring, R. F. *J. Chem. Phys.* **1999**, *111*, 9754.
- (12) Lee, J. Y.; Baljon, A. R. C.; Sogah, D.; Loring, R. F. *J. Chem. Phys.* **2000**, *112*, 9112.
- (13) Valignat, M. P.; Oshanin, G.; Villette, S.; Cazabat, A. M.; Morceau, M. *Phys. Rev. Lett.* **1998**, *80*, 5377.
- (14) de Gennes, P. G.; Cazabat, A. M. *C. R. Acad. Sci. (Paris)* **1990**, *310*, 1601.
- (15) Kremer, K.; Grest, G. S. *J. Chem. Phys.* **1990**, *92*, 5057.
- (16) Doi, M.; Edwards, S. F. *The Theory of Polymer Dynamics*; Oxford Press: Oxford, 1986.
- (17) Evans, K. E.; Edwards, S. F. *J. Chem. Soc., Faraday Trans. 2* **1981**, *77*, 1891.

MA010405J